Review

Earliest Evolved Rocks: A Solar System Perspective

Sheng Shang *

Posted Date: 19 January 2026

doi: 10.20944/preprints202601.1308.v1

Keywords: evolved rocks; early crust; Moon; Mars; asteroid; solar system

 doi:10.20944/preprints202601.1308.v1

Review

Earliest Evolved Rocks: A Solar System Perspective

Sheng Shang

Center for High Pressure Science and Technology Advanced Research, Beijing 100193, China; sheng.shang@hpstar.ac.cn

Abstract

Granitic rocks dominate Earth's continental crust, yet the Hadean record is severely limited. Extraterrestrial evolved lithologies, crystallized under anhydrous, plate tectonics-free conditions analogous to those of early Earth, provide valuable analogues. This review synthesizes lunar, asteroidal, Martian, and candidate Venus/Mercury data, revealing that partial melting of mafic protoliths, not fractional crystallization or silicate liquid immiscibility, represents the dominant formation mechanism. Granitic magmatism persisted episodically from merely 2.3 Myr after Solar System formation through at least 3.87 Ga, with estimated abundances of 0.2–2% representing a conservative lower limit. These findings imply that Hadean Earth possessed the thermal and compositional prerequisites for analogous magmatism, potentially yielding a crustal inventory of 0.2–40% felsic material. By establishing a comparative planetary framework, this study illuminates pathways for reconstructing Earth's earliest crustal evolution and highlights priorities for future exploration missions targeting cryptic silicic reservoirs, particularly deep-crustal exposures in large lunar impact basins and in situ characterization of Venusian highland terrains.

Keywords: evolved rocks; early crust; moon; mars; asteroid; solar system

1. Introduction

Earth's continental crust constitutes the principal archive of geological, geochemical, and biological evolution, yet the mechanisms governing its formation during the Hadean eon (4.56–4.0 Ga) remain profoundly enigmatic [1–4]. Evolved rocks, broadly defined here as lithologies exceeding 52 wt.% SiO_2 to encompass intermediate to felsic compositions [5], dominate the upper crust and has long been considered unique to Earth among planetary bodies. Deciphering its petrogenesis is therefore essential for reconstructing crustal growth, particularly during primordial epochs when nascent conditions diverged fundamentally from those prevailing today.

Direct investigation of Hadean granites is severely hampered by terrestrial preservation biases. The only mineralogical vestiges are detrital zircons from Jack Hills, Western Australia, whose Ti-in-zircon thermometry and trace-element systematics indicate crystallization from granitic protoliths as old as ~4.4 Ga [3,6,7]. The oldest intact rocks, the ~4.0 Ga Acasta Gneisses [8,9], similarly attest to early granitic activity, yet their extreme rarity and ambiguous tectonic contexts preclude robust assessment of Hadean crustal characteristics. Critically, the most abundant terrestrial granitoids are Archean tonalite-trondhjemite-granodiorite (TTG) suites, whose petrogenesis is intimately linked to plate tectonics and hydrous melting [10–12]. However, the relationship between TTG and Hadean granites remains unresolved, rendering TTG alone insufficient for reconstructing Earth's primordial crustal evolution and necessitating alternative analogues.

Extraterrestrial evolved rocks provide uniquely valuable analogues for early Earth, as they formed under ancient, anhydrous, and plate tectonics–free conditions comparable to those prevailing on the Hadean Earth [13–16]. No evidence for plate tectonics has been observed beyond Earth, and these lithologies conspicuously lack hydrous minerals such as amphibole and biotite, attributes that starkly contrast with TTG petrogenesis. This review synthesizes recent discoveries across the Solar System, integrating sample analyses, in-situ rover measurements, and orbital remote-sensing

 doi:10.20944/preprints202601.1308.v1

observations from the Moon, asteroids, Mars, Venus, and Mercury. We first present body-specific advances, then compare petrologic and geochemical characteristics across planetary bodies, and finally evaluate implications for understanding Earth's earliest granitic crust, thereby establishing a comparative planetary framework that illuminates pathways for reconstructing Hadean crustal evolution and highlights priorities for future exploration missions targeting cryptic felsic reservoirs.

2. The Moon

2.1. Lunar Samples

Lunar granites are exclusively preserved as lithic clasts within impact breccias, a mode of occurrence that fundamentally distinguishes them from their terrestrial counterparts. Unlike Earth's extensive granite batholiths and volcanic complexes that outcrop at the surface, silicic clasts on the Moon occur only as isolated fragments exhumed by impact gardening [17,18]. These clasts constitute volumetrically minor components of the lunar crust, yet their survival in the regolith provides unprecedented insights into ancient magmatic processes operating under anhydrous, plate tectonics-free conditions.

Mineralogically, lunar granites are dominated by calcic plagioclase, quartz, and K-feldspar (Figure 1), with subsidiary but significant mafic phases including fayalitic olivine, pyroxene, ilmenite, zircon, and phosphates (apatite, merrillite) [18,19]. The conspicuous absence of hydrous minerals such as amphibole and biotite starkly contrasts with terrestrial granitoids and underscores the anhydrous nature of lunar magmatism [18]. Texturally, these rocks display characteristic granophyric intergrowths of quartz and feldspar, manifested as vermicular microstructures with crystal continuity extending up to 1.8 mm in the coarsest samples [17]. This texture reflects rapid, near-surface crystallization of highly viscous, silica-rich melts.

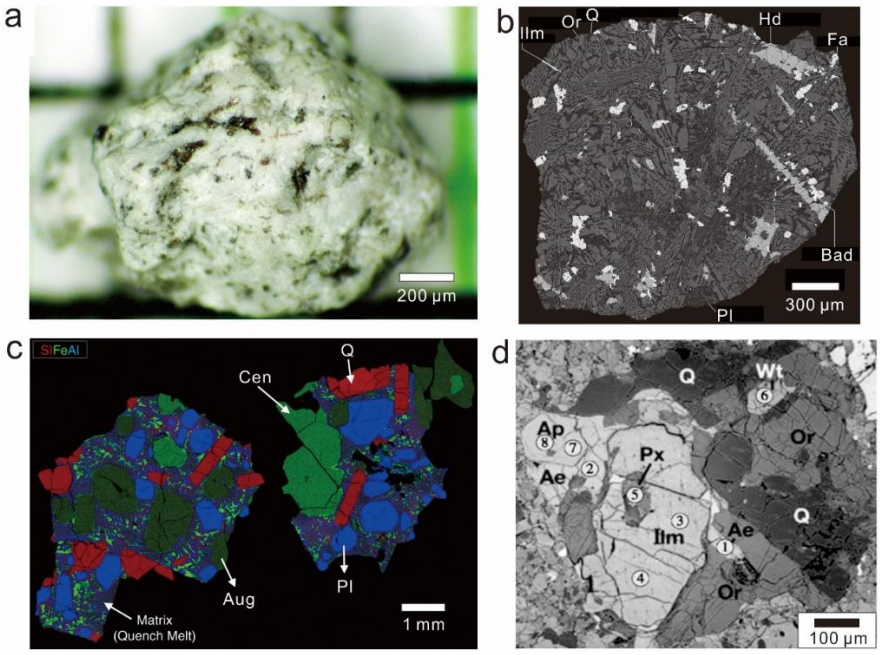

Figure 1. Representative morphological and textural characteristics of typical extraterrestrial evolved materials in specimen . (a) Optical photograph and (b) backscattered electron (BSE) image of the lunar silicic clast 12032, 366-19, illustrating its characteristic light-colored macroscopic appearance and microscopic granophyric intergrowth (Modified from Seddio et al., 2013). (c) False-colored X-ray map of the achondrite NWA 11119, depicting an evolved mineral assemblage (Modified from Srinivasan et al., 2018). (d) BSE image of a granitic clast within the Adzhi-Bogdo ordinary chondrite regolith breccia, featuring an anhydrous mineral assemblage

 doi:10.20944/preprints202601.1308.v1

(modified from Terada and Bischoff, 2009). Ap = Apatite, Ae = Aenigmatite, Ilm = Ilmenite, Wt = Whitlockite, Q = Quartz, Or = K-feldspar.

High-precision geochronology constrains lunar granite crystallization to an episodic 500 Myr interval from 4.37 to 3.87 Ga [5,13]. Pb-Pb and K-Ca dating of twelve clasts resolved eight distinct age peaks, precluding direct derivation from lunar magma ocean (LMO) crystallization and instead requiring post-primary-crust magmatic processes [13]. This protracted duration demonstrates that silicic magmatism was not a singular event but a recurrent phenomenon throughout the Moon's early thermal evolution.

Granitic clasts have been recovered from multiple Apollo landing sites, with Apollo 14 yielding the highest concentration [20]. Notable specimens include the largest pristine clast (14321,1027), which measures 16 mm × 7 mm with a mass of 1.8 g and exhibits ultra-low siderophile element abundances (Ir < 3×10^{-4} × CI chondrite) confirming its endogenous origin [17]. Modal abundance estimates based on regolith compositions suggest granite may constitute 0.5–2% of the lunar crustal volume [20], establishing a critical baseline for comparative planetary analysis.

2.2. Orbital Observations

Orbital remote-sensing data provide crucial complementary constraints on the distribution and lithology of lunar silicic magmatism, revealing volcanic constructs that are far too voluminous to be sampled by random regolith processes. The lunar surface hosts numerous silicic domes, including Gruithuisen and Mairan, Hansteen Alpha, and the farside Compton-Belkovich anomaly, characterized by high albedo, 400–600 m topographic relief, and steep 20–26º flank slopes [21,22]. These morphological attributes, analogous to terrestrial rhyolitic domes, signal eruption of highly viscous, silica-rich magmas.

Mid-infrared spectroscopy from the Diviner Lunar Radiometer provides definitive mineralogical confirmation, detecting a short-wavelength Christiansen Feature (7.1–8.6 μm) diagnostic of highly polymerized silica phases including quartz, alkali feldspar, and silica-rich glass [21]. This spectral signature correlates with pronounced incompatible element enrichment in gamma-ray data: K, Th (typically 40–60 ppm, locally >10 ppm at Compton–Belkovich), and U are elevated while FeO and TiO_2 are depleted [22]. The Th enrichment, in particular, serves as a robust orbital proxy for silicic lithologies [22] and directly aligns with geochemical patterns observed in Apollo granite clasts [18].

This magmatism occurred in both extrusive and intrusive facies, as evidenced by morphological diversity spanning >6 km domes to <1 km constructs and arcuate collapse depressions [22]. Such variation implies that substantial granite plutons remain undiscovered within the lunar interior. The most viable generation mechanism involves basaltic underplating of KREEP-enriched crust, partial melting of anorthositic wall rocks, and gravity-driven segregation of buoyant silicic melts [23]. This model is reinforced by orbital gamma-ray data showing a longitudinal K-Th-U concentration between 0º and 50º W [24]—the same region where Apollo 12 and 14 recovered enriched granite clasts—demonstrating that orbital compositional anomalies faithfully map ancient silicic magma systems.

2.3. Petrogenesis

The petrogenesis of lunar granites remains vigorously debated despite decades of study, with three competing mechanisms including fractional crystallization, silicate liquid immiscibility, and crustal partial melting, each facing distinct theoretical and observational challenges. Resolving this controversy is essential for understanding how silicic magmatism operates in anhydrous planetary bodies.

Fractional crystallization of KREEP basaltic magma can generate residual melts enriched in silica and incompatible elements, but thermodynamic modeling demonstrates severe volumetric limitations. This process yields ≤15% residual liquid and fails to produce the high SiO_2 contents (~70

 doi:10.20944/preprints202601.1308.v1

wt%) observed in lunar granites before sufficient melt remains for viable extraction [23]. Furthermore, crystallization-age distributions showing eight distinct peaks over 500 Myr [13] are inconsistent with a simple differentiation trend from a single parental magma.

Silicate liquid immiscibility faces more fundamental geochemical contradictions. While experimental studies confirm that residual melts after 90–98% crystallization can separate into Si-rich and Fe-rich conjugate liquids [25,26], high-field-strength elements partition preferentially into the mafic melt ($D_{mafic/felsic}$ ~5.6 at 1000 ºC) [23]. This directly contradicts the observed Th enrichment (20–70 ppm) in both granite clasts and silicic domes [22]. Although microscopic immiscibility textures occur in some samples, the required complementary Fe-rich, Th-enriched reservoir has never been identified, indicating this mechanism was at most subordinate.

Crustal partial melting emerges as the most viable mechanism. Experimental partial melting of monzogabbro protoliths at 1000 °C produces Si-rich melts (~68 wt% SiO_2) whose weighted bulk composition matches lunar granites, provided immiscibility is suppressed at crustal depths (>0.005 GPa) [23]. This model can generate substantial melt fractions (~40%) capable of forming both intrusive plutons and extrusive domes, consistent with the observed petrologic diversity and Th enrichment. Basaltic underplating of KREEP-rich lower crust provides both the heat source and fertile source composition [21,23]. However, definitive resolution requires high-pressure experiments quantifying trace-element partitioning under lunar oxygen fugacity conditions and modeling melt extraction dynamics from partially molten anorthositic crust.

3. Asteroids

Beyond lunar samples, recent investigations have increasingly identified evolved materials in non-lunar meteorites [14–16,27–31]. These materials predominantly derive from the asteroid belt and preserve both chondritic [14] and primitive achondritic affinities [15,16,28–31]. Occurrences span meteorites with bulk evolved compositions [16,27–29,31] to isolated evolved clasts within polymict breccias [15,30]. All formed under ancient, anhydrous, plate tectonics–free conditions.

3.1. Chondrite

The occurrence of evolved lithologies within chondrites, the primitive meteorites that escaped large-scale melting, presents a fundamental paradox: it requires localized, high-temperature magmatism on bodies that never achieved global differentiation. The LL3-6 ordinary chondrite regolith breccia Adzhi-Bogdo resolves this paradox, preserving multiple granitic clasts that crystallized under anhydrous conditions fundamentally distinct from those governing lunar or terrestrial granites [14,32].

Mineralogical evidence demands slow cooling in a large-scale magma reservoir. These clasts contain quartz (26 vol.%), K-feldspar (Or_{95}; 35 vol.%), aenigmatite (9 vol.%) and ilmenite (21 vol.%), with crystal sizes reaching 700 μm within ~800 μm clasts (Figure 1) [14]. Such coarse-grained textures are incompatible with rapid quenching expected from impact melting. Oxygen isotope systematics plot within the ordinary chondrite field, confirming formation on a parent body with chondritic compositional affinities rather than exotic provenance [33].

Pb-Pb dating of co-genetic phosphates yields a weighted mean age of 4.53 ± 0.03 Ga, establishing these as the ancient known evolved materials, predating lunar granites by ~100 Myr [14]. This antiquity, combined with the thermal evolution recorded in the host meteorite, precludes impact-generated melting and instead points to ^{26}Al radioactive heating as the viable energy source. The implication is profound: granitic magmatism may have been a widespread, intrinsic process during early planetesimal evolution, occurring even on bodies that did not undergo full-scale differentiation.

3.2. Achondrite

Primitive achondrites preserve bulk-granitic lithologies that provide crucial insights into early Solar System magmatism beyond the fragmentary record of chondritic clasts. Unlike xenolithic

 doi:10.20944/preprints202601.1308.v1

materials, these specimens represent intact samples of evolved crust from partially differentiated parent bodies, establishing a paradigm for rapid asteroidal crustal evolution.

Erg Chech 002 (EC 002) is the most ancient known igneous rock, crystallizing at 4565.0 Ma—merely 2.3 Myr after Solar System formation [27]. Its porphyroblastic texture (1–1.5 mm matrix, cm-scale phenocrysts) and mineralogy (45–50 vol% albitic plagioclase An_{6-22}, 38–45 vol% augite, 5 vol% cristobalite/tridymite) resemble terrestrial andesites but preserve high-temperature SiO_2 polymorphs. The bulk composition (58–59.5 wt% SiO_2, Mg# 52–53, 4.2 wt% Na_2O) and flat REE pattern indicate ~25% partial melting of a non-carbonaceous chondritic source at IW-1.38 and ~1220 °C [34]. Elevated $\delta^{26}Mg$ values reveal a protracted melting-to-crystallization interval of 10^5–10^6 years, reflecting sluggish migration of high-viscosity melt in a partially differentiated body [27]. This demonstrates that post-differentiation silicate remelting generated evolved lithologies within the first few million years of planetesimal accretion.

The brachinite Graves Nunataks 06128/9, the first bulk-evolved achondrites recognized [28], crystallized at 4.517 ± 0.060 Ga. These rocks contain 54.6–57.6 wt% SiO_2 and are dominated by plagioclase (>75 vol%, An~14) with olivine, pyroxene, phosphates, and sulfides, signaling volatile enrichment [29]. Pyroxene exsolution textures indicate shallow crustal emplacement (15–20 m depth) [28]. Experimental petrology corroborates generation via low-degree partial melting of a volatile-rich chondritic protolith, establishing that granitic crust formation was operative within <100 Myr of Solar System inception.

Ureilite-affiliated meteorites ALM-A and NWA 11119 provide complementary perspectives on a single parent body. ALM-A (60.07 wt% SiO_2, 6.88 wt% alkalis) consists of ~70 vol% plagioclase (An_{10-55} and An_{5-12}) with bimodal pyroxenes, crystallizing at 4561 Ma [31]. NWA 11119 (61.37 wt% SiO_2, 0.93 wt% alkalis) is distinguished by ~30 vol% tridymite, the highest free-silica abundance in meteorites (Figure 1), dated at 4564.8 ± 0.3 Ma (Figure 2) [16]. The ~3.5 Myr age gap and contrasting alkali contents reflect either source heterogeneity or melt extraction efficiency, indicating sustained granitic activity across varied crustal levels during asteroid assembly [16,31].

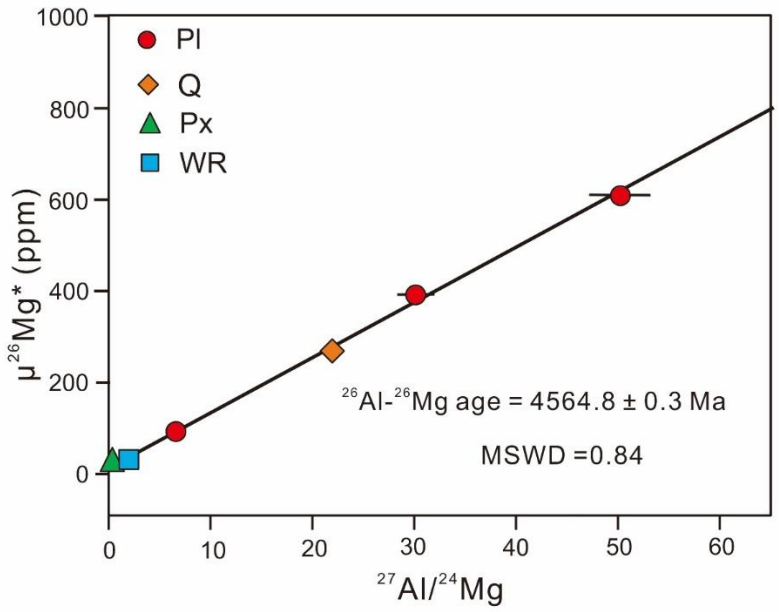

Figure 2. Internal ^{26}Al-^{26}Mg isochron of the silica-rich achondrite NWA 11119 (Modified from Srinivasan et al., 2018). The regression line, calculated from plagioclase (Pl), quartz (Q), pyroxene (Px), and whole-rock (WR) fractions, yields a high-precision crystallization age of 4564.8±0.3 Ma with a Mean Square Weighted Deviation (MSWD) of 0.84.

In contrast, the ureilite EET 87720 preserves granitic clasts of foreign origin that demonstrate impact mixing. O-isotope compositions overlap H chondrites and IIE irons, decoupled from the host

 doi:10.20944/preprints202601.1308.v1

ureilite [15]. The clasts comprise quartz, albite, high-silica glass (72 wt% SiO_2), and granophyric intergrowths, with a bulk composition reaching 77 wt% SiO_2—suggesting extreme fractional crystallization or very low-degree melting [15]. However, fine grain sizes and ambiguous provenance preclude definitive constraints on source melting conditions.

Collectively, these achondrites demonstrate that granitic magmatism occurred across diverse thermal and compositional regimes, from rapid melting of pristine chondritic material to remelting of differentiated crust, and operated continuously from the earliest Solar System through the assembly of large asteroids.

3.3. Vesta

As the largest differentiated asteroid (525 km diameter), Vesta possesses a well-characterized basaltic primary crust (eucrites) and ultramafic mantle (diogenites), making it a critical test case for secondary crustal melting processes. Howardites, which are polymict breccias sampling this crust, provide the only direct material record of Vestian surface lithologies. The discovery of evolved compositions within this suite would confirm whether tertiary crust formation—partial melting of primary basaltic materials—operates at this intermediate planetary scale.

The howardite pairing group Dominion Range 2010 (DOM 10) contains a 4 mm dacitic clast in sample DOM 10100,8 that represents the first characterized sample of Vesta's tertiary crust [30]. This clast exhibits a primary igneous assemblage dominated by plagioclase, augite, and quartz (~30 vol%), with subsidiary pigeonite, ilmenite, Fe-Ni metal, troilite, phosphates, and K-feldspar. The crystalline texture and mineralogical maturity indicate slow cooling within a substantial melt body rather than quenching of impact melt.

Thermodynamic and trace-element modeling corroborate a crustal melting origin. MELTS simulations demonstrate that 10-20% equilibrium partial melting of a Juvinas-type basaltic crust at 200 bars reproduces the dacite's major-element composition and mineralogy, while quantitative trace-element modeling matches its enriched incompatible element signature [30]. This establishes that partial melting of a basaltic primary crust, a process directly analogous to terrestrial continental crust formation, operated on Vesta, producing volumetrically minor but geochemically significant evolved melts that complement the basaltic and cumulate lithologies preserved in the meteorite record.

This discovery extends the crustal melting mechanism to asteroidal scales, demonstrating that bodies intermediate in size between small achondrite parent bodies and the Moon can generate evolved magmas. While volumetrically minor compared to Vesta's dominant basaltic crust, these evolved melts are geochemically significant as they represent the first confirmed products of secondary differentiation on a large asteroid. The operating mechanism, partial melting of primary basaltic crust, mirrors processes proposed for the Moon and Mars, establishing this as a universal pathway for generating evolved magmas across planetary bodies with basaltic lithospheres.

4. Mars

4.1. Martian Meteorites

The Martian breccia meteorite NWA 7034 and its paired stones (e.g. NWA 7533, NWA 8171) provide the only direct samples of Mars' ancient crust beyond the dominantly basaltic SNC suite, preserving a record of crustal evolution that challenges the long-standing paradigm of a uniformly mafic Martian lithosphere [35,36]. Unlike the SNC meteorites, which sample young volcanic surfaces, this breccia suite contains lithic clasts derived from the ancient Noachian crust, offering a unique window into early Martian differentiation.

NWA 7034 preserves highly varied clast compositions and textures. Some coarse-grained clasts are dominated by plagioclase, alkali feldspar, and apatite; however, because individual mineral grains reach hundreds of micrometers, these clasts typically contain only three to four mineral grains, precluding definitive protolith identification [36]. Nevertheless, these mineral assemblages likely

 doi:10.20944/preprints202601.1308.v1

originated from evolved parent rocks. Fine-grained clasts include trachyandesitic and basaltic andesitic lithologies with ~54 wt.% SiO_2, which is substantially more evolved than typical Martian basalts (45–52 wt.% SiO_2) and extending the known compositional range of Martian magmatism [35].

Recent discoveries provide unequivocal evidence for granitic components. Lindner et al. (2020) identified a ~170 μm granitic clast in NWA 8171 composed of quartz, plagioclase, and alkali feldspar with minor apatite, zircon, and magnetite—an assemblage analogous to terrestrial granite [37]. More significantly, Malarewicz et al. (2025) documented multiple quartz-bearing clasts in NWA 7533 representing the most silicic Martian lithologies yet recognized. These clasts exhibit granitic compositions exceeding 70 wt.% SiO_2, with quartz grains showing crystalline Raman signatures, homogeneous cathodoluminescence, and minor shock features consistent with a magmatic origin rather than shock metamorphism [38]. The Hf isotopic compositions of zircons in NWA 7034 may further record andesitic crustal information dating back to 4.547 Ga, providing direct evidence for evolved crust formation within the first 100 Myr of Martian history [39].

Thus, the NWA 7034 suite preserves multiple, independent signals of granitic material. However, the rare, fine-grained, and fragmented nature of these clasts limits their discovery and detailed investigation. The bulk composition of this ancient breccia is andesitic overall, indicating that evolved lithologies were interspersed with dominant basaltic crust. These meteorite data establish that Mars possessed the compositional prerequisites for granite formation, but the sparse sampling underscores the need for in situ rover observations to assess regional distributions and petrogenetic contexts.

4.2. Rover Observations

In situ investigations by the Curiosity rover at Gale crater provide unique textural and mineralogical constraints unattainable through orbital or meteorite studies, establishing that Noachian Mars (~3.6–4.1 Ga) hosted diverse felsic lithologies that challenge the paradigm of a uniformly basaltic crust [40]. These ground-truth observations are critical because they preserve magmatic textures and mineral assemblages that would be destroyed or obscured during impact ejection and atmospheric entry.

The landmark discovery of tridymite in the Buckskin drill sample of the Murray Formation provides the first definitive mineralogical evidence for silicic magmatism on Mars (Morris et al., 2016). This high-temperature (>870 ºC), low-pressure SiO_2 polymorph occurs in laminated lacustrine mudstone with ~74 wt.% SiO_2, comprising ~40 wt.% crystalline material (plagioclase, tridymite, sanidine, magnetite, cristobalite) and ~60 wt.% amorphous silica-rich phases. On Earth, tridymite forms exclusively through silicic volcanism, vapor-phase crystallization in ash-flow tuffs, or high-temperature metamorphism. Its occurrence in finely laminated sediments therefore implies derivation from eroded rhyolitic sources in the crater rim or central uplift, confirming that by the Noachian, Mars had attained both the thermal conditions and compositional prerequisites for generating high-silica melts.

ChemCam remote microanalyses further resolve three distinct felsic-to-intermediate rock groups in the Bradbury landing site vicinity, extending the compositional range of Martian magmatism to 64–72 wt.% SiO_2 and total alkalis of 4.5–14 wt.% [40,41]: (1) Coarse-grained granodiorite/quartz-diorite with >5 mm andesine-quartz intergrowths, diagnostic of slow-cooled plutonic emplacement; (2) Aphanitic trachyte with glassy matrices (<100 μm) and conchoidal fractures, consistent with effusive volcanism; and (3) Porphyritic trachyandesite containing cm-scale oligoclase phenocrysts, indicating intermediate intrusion depths. These lithologies are interpreted as Noachian-aged analogs to terrestrial TTG suites, representing the first in situ confirmation of continental-type crust on another planetary body.

Independent evidence corroborates this paradigm shift. Reevaluation of Mars Pathfinder andesitic compositions suggests a primary magmatic origin (Sautter et al., 2016), while gravity data imply southern highlands crustal densities (2.7–3.1 g/cm^3) significantly lower than basaltic meteorites (3.1–3.3 g/cm^3) [42,43]. Collectively, these multi-scale observations converge on a model where

 doi:10.20944/preprints202601.1308.v1

granitoid magmatism constitutes a previously cryptic component of Mars' early crust, formed through low-degree partial melting of a K-rich mantle and subsequent fractional crystallization at low pressure [40].

4.3. Orbital Observations

Orbital remote-sensing data provide the only means to assess the global distribution of evolved lithologies on Mars, complementing the localized perspectives of rover and meteorite studies. However, orbital observations fundamentally underestimate granite abundances due to intrinsic spectral limitations and surficial overprinting effects.

Thermal Emission Spectrometer (TES) and THEMIS data identified a dacitic volcano at Nili Patera caldera, while CRISM analyses revealed felsic outcrops in Xanthe Terra, Syrtis Major, and Northeast Noachis Terra [44,45]. These discoveries confirm that evolved magmatism occurred regionally, not merely as isolated clasts. However, detection is severely biased: feldspar exhibits only weak ~1.3 μm absorptions from minor Fe^{2+} substitution and becomes undetectable when mafic mineral modes exceed ~5 vol%, a threshold above which pyroxene and olivine dominate the spectrum [41,45]. Since Martian crust contains ubiquitous mafic components, many felsic bodies likely remain spectrally masked.

This detection bias is compounded by thick, spectrally opaque regolith from impact gardening and global dust storms, causing orbital measurements to reflect surface cover rather than underlying bedrock lithology [41]. Consequently, mapping granite exposures requires robust discrimination of bedrock signatures from overprinting materials. Notably, orbitally detected occurrences exhibit high thermal inertia and negligible dust cover, implying numerous additional felsic bodies remain cryptic within the Martian crust, particularly in dust-mantled highland regions where in situ observations are unavailable.

5. Venus and Mercury

In contrast to the Moon, asteroids, and Mars, relatively limited information is available for Venus and Mercury. Nevertheless, existing data suggest that both planets may host abundant evolved lithologies, although these occurrences remain unverified. Confirmation of evolved rocks on Venus and Mercury would profoundly impact our understanding of evolved magmatism across the Solar System.

5.1. Venus

Venus emerges as the critical test case for granite formation beyond Earth precisely because its Earth-like size and thermal budget operate without plate tectonics, potentially capturing a transitional geodynamic regime between early Solar System plutonism and full-fledged subduction. Long-lived magmatic activity has resurfaced the planet, yielding a youthful crustal age of only ~500 Myr [46], while mantle plumes provide sustained crustal heating [47]. Although Venus's early habitable conditions and subsequent desiccation differ fundamentally from the anhydrous Moon [48], the planet's thermal evolution may have generated evolved magmatism through mechanisms analogous to thickened plateau melting on early Earth.

Orbital spectral data provide the first line of evidence. Near-infrared emissivity measurements from the Galileo Near-Infrared Mapping Spectrometer reveal systematically lower values in Venusian highlands relative to lowland regions [48]. This spectral contrast is difficult to reconcile with mafic lithologies alone and strongly suggests felsic, potentially granitic compositions in highland terrains. The emissivity anomaly is geographically correlated with ancient tesserae, the most heavily deformed and isostatically compensated crust, implying that these high-standing plateaux may represent thickened, compositionally evolved crust analogous to terrestrial continental nuclei.

 doi:10.20944/preprints202601.1308.v1

Morphological evidence reinforces this interpretation. A globally distributed population of pancake-shaped domes, steep-edged, flat-topped volcanoes 10–100 times larger than terrestrial counterparts, implies eruption of highly viscous, silicic magma [49,50]. The domes' dimensions and aspect ratios are consistent with compositions exceeding 65 wt% SiO_2, requiring significant crustal melting rather than fractional crystallization alone. Their stratigraphic association with corona-like structures further suggests a genetic link to mantle plume activity, wherein plume-induced crustal underplating drives partial melting of hydrated basaltic lower crust.

In situ geochemical measurements from Venera and Vega landers provide direct, albeit limited, support. XRF analyses identified K_2O-rich compositions at Venera 8 (4.8 ± 1.4 wt.%) and Venera 13 (4.1 ± 0.63 wt.%) landing sites [51]. When interpreted within their geologic context—the landers sampled highland plateaux—these potassium enrichments suggest differentiated, potentially granitic lithologies [52]. Collectively, these multi-scale observations converge on a scenario where Venusian highlands represent felsic plateaux formed through partial melting of hydrated basaltic crust in a plume-driven environment, offering a potential analogue for pre-plate-tectonic Earth.

5.2. Mercury

Mercury's prolonged magmatic activity makes it a critical end-member for evaluating granite formation on small planetary bodies. Unlike the Moon, whose volcanism ceased by ~2 Ga, Mercury's most recent eruptions may date to ~1 Ga [53], providing a substantially extended thermal window for crustal melting. This longevity potentially compensates for Mercury's limited radiogenic heat production, raising the prospect of secondary magmatism on a body otherwise dominated by primary crust formation.

Remote observations suggest Mercury's surface is compositionally evolved. The planet's high albedo and low $FeO+TiO_2$ contents (<6 wt.%) measured by microwave and mid-infrared spectroscopy imply limited mafic lithologies and feldspar abundances comparable to lunar highlands [54]. However, distinguishing feldspar from quartz spectroscopically is challenging [41], leaving open the possibility that Mercury's surface may be quartz-enriched. Combined with the existence of lunar granites, Mercury's spectrally analogous surface suggests that granite could occur on this anhydrous body, albeit likely as mafic-rich, lunar-style lithologies rather than terrestrial hydrous granitoids.

Ultimately, Mercury represents an end-member case between the Moon (small, volcanically dead) and Venus (large, geologically active). The fundamental question is whether its extended magmatism generated sufficient heat for crustal anatexis despite its limited size. This remains unresolved pending high-resolution orbital compositional data that can discriminate felsic lithologies from the mafic background.

6. Granitic Systematics

Evolved materials occur across diverse planetary bodies, yet extraterrestrial evolved rocks exhibit significant heterogeneity in petrography, geochemistry, chronology, and petrogenesis. These differences are critical for deciphering granitic magmatism throughout the Solar System. Notably, extraterrestrial evolved samples provide unambiguous constraints on mineralogical, geochemical, and chronological information (Table 1).

Table 1. Mineralogical, geochemical, and geochronological characteristics of representative extraterrestrial evolved lithologies from across the Solar System. (Ol = Olivine, Px = Pyroxene, Pl = Plagioclase, Kfs = Potassium feldspar, Ae=Aenigmatite, IW= Iron-wüstite).

Sample	Lunar evolved rock	NWA 11119	ALM-A	EC002	EET 87220	Adzhi-bogdo	GRA 06128/9	DOM 10	NWA 7034

 doi:10.20944/preprints202601.1308.v1

Major mineral	Ol、Px、Pl、Kfs、Q	Px、Pl、Q	Px、Pl、Q	Pl、Px、Q	Pl、Q	Kfs、Q、Ae	Ol、Px、Pl	Px、Pl、Kfs、Q	Px、Pl、Q
Mineral size	<~500 μm	~1-~4 mm	~0.2-~2 mm	~0.2->10 mm	<~100 μm	~100-~500 μm	~0.1-~1 mm	~0.1-~1 mm	<~100 μm
An of Pl	~35-~85	~65-~92	~5-~55	6.7-21.6	~0-~12	-	~13-~14	~86	23-41
Or of Kfs	~88-~98			84.0-84.4		~96-~97		~97	65-92
Bulk SiO_2	>53	~59-~62	60	58	77	72-78	52-58	54.5	53-77
Bulk Mg#	0-62	64-85	61	53	0	15-47	28-39	23	26-58
Bulk K_2O/Na_2O	1-13	~0	0.03	0.08	0.10	3.21-18.63	0.30	0.09	0.05-1.48
fO_2	< IW	< IW	-	<IW	-	-	IW to IW+1	IW	-
Age（Ga）	3.88-4.32	4.565	4.561	4.5659	-	4.533	4.52	-	4.4
Parent body	The Moon	Ureilite	Ureilite	Ungrouped Chondrite	-	Ordinary Chondrite	Brachinite	Vesta	Mars

6.1. Petrology, Geochemistry, Chronology

Extraterrestrial evolved rocks exhibit remarkable mineralogical heterogeneity that fundamentally distinguishes them from terrestrial granitoids. Unlike Earth's granites, which are predominantly quartz- and K-feldspar-rich, extraterrestrial samples ubiquitously incorporate mafic minerals: fayalitic olivine and pyroxene occur as essential constituents in lunar granites and the brachinite GRA 06128/9 [18,28,55], while pyroxene is nearly universal across achondrites except for the ureilite EET 87720 and Adzhi-Bogdo chondritic clasts [14,15]. Modal variations are dramatic—NWA 11119 is quartz-dominated [16], ALM-A is plagioclase-rich [31], while K-feldspar is restricted to select lithologies (Adzhi-Bogdo, DOM 10) and quartz is absent from GRA 06128/9 [28,30]. Grain sizes span three orders of magnitude (100 μm–10 mm), reflecting crystallization in contrasting thermal regimes and magma chamber scales (Figure 1, Table 1).

Chemical systematics reveal a compositional spectrum spanning andesitic to felsic and alkaline to subalkaline series (Figure 3). Elevated FeO and MgO reflect mafic mineral components, with Mg# ranging from near-zero to ~60 and plagioclase compositions spanning An_{90} to An_{10} [27,31]. Na_2O/K_2O ratios straddle unity, indicating divergent alkali fractionation paths. Despite S- and Cl-rich volatile phases in some samples (ALM-A, EET 87720, GRA 06128/9, DOM 10), their absence elsewhere demonstrates fluxing agents are not requisite [28–30]. Oxygen fugacity spans several log units below to marginally above the iron-wüstite buffer [29], while Eu anomalies vary from positive to negative (Figure 4), reflecting diverse plagioclase fractionation histories and source heterogeneity.

Chronological data document both primordial bursts and sustained activity. Erg Chech 002 crystallized at 4565.0 Ma, merely 2.3 Myr after Solar System formation, demonstrating that silicic crustal generation initiated within the first few million years of planetesimal accretion [27]. Ureilites NWA 11119 and ALM-A crystallized 3.5 Myr apart on a shared parent body [16,31], indicating sustained granitic production during asteroid assembly. Lunar granite clasts preserve 500 Myr of

 doi:10.20944/preprints202601.1308.v1

episodic magmatism (4.37–3.87 Ga), documenting persistent silicic activity long after terrestrial planet formation [13]. Collectively, these temporal constraints reveal granitic magmatism as both a transient early Solar System phenomenon and an enduring planetary process.

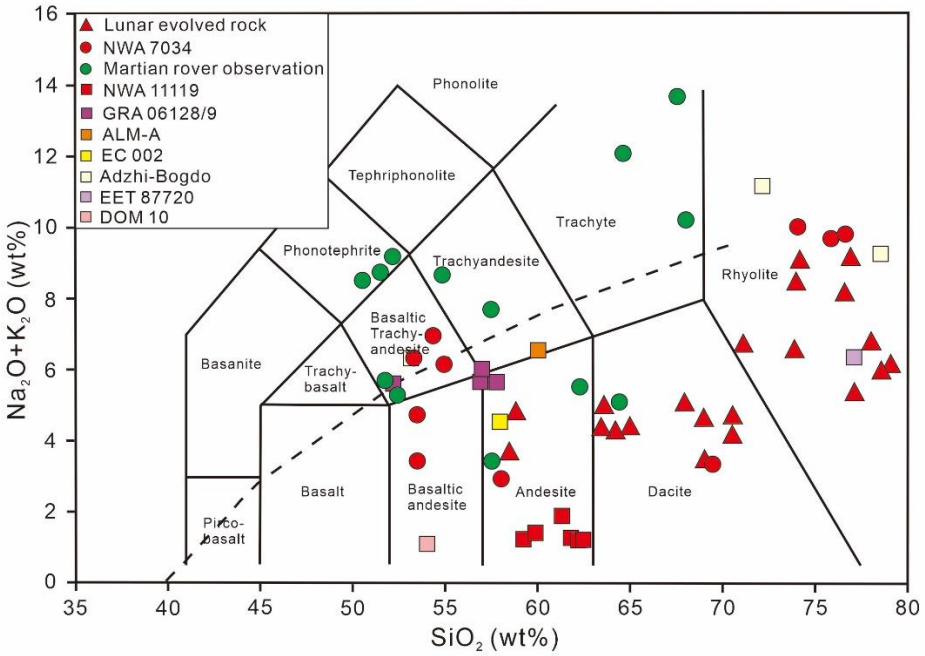

Figure 3. Total alkali versus silica (TAS) diagram illustrating the major-element chemical diversity of extraterrestrial evolved lithologies across the Solar System. The data demonstrate a profound chemical heterogeneity, with samples spanning from andesitic to felsic compositions and straddling both the alkaline and subalkaline series. This broad distribution includes lunar granitic clasts, Martian components documented via the NWA 7034 breccia suite and in-situ Curiosity rover observations, and a diverse array of asteroidal meteorites, including ureilitic (NWA 11119, ALM-A, EET 87720), brachinitic (GRA 06128/9), chondritic (Adzhi-Bogdo), and vestan (DOM 10) samples.

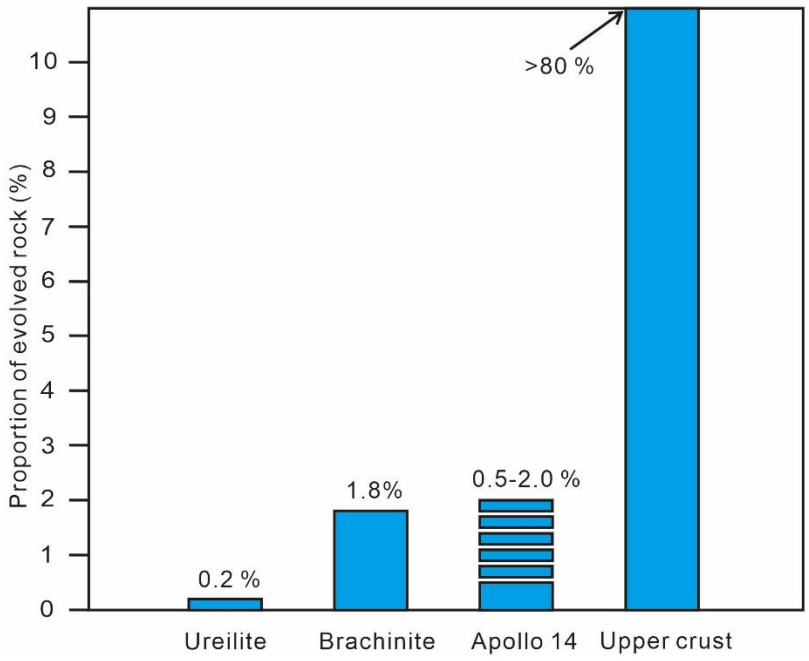

 doi:10.20944/preprints202601.1308.v1

Figure 4. Comparative abundance of granitic lithologies across the Solar System relative to Earth's upper crust. The estimated proportions of evolved rocks—0.2% for ureilites , 1.8% for brachinites , and 0.5–2.0% for the Apollo 14 lunar regolith, are contrasted with the >80% felsic dominance of Earth's modern upper crust.

6.2. Dominant Petrogenesis

Building upon the lunar case detailed in Section 2.3, extraterrestrial granites across the Solar System exhibit a consistent petrogenetic pattern: partial melting of mafic protoliths dominates, while fractional crystallization and silicate liquid immiscibility remain volumetrically subordinate. However, the specific manifestation of partial melting varies systematically with parent body size, thermal architecture, and redox conditions, establishing a comparative framework that illuminates the fundamental controls on evolved magmatism in anhydrous environments.

Asteroidal-scale melting (bodies <1000 km diameter) operated on chondritic protoliths during the earliest Solar System. Experimental studies demonstrate that <30% partial melting of chondritic material at IW-2 to IW-1 generates granitic liquids, with progressively lower melting degrees yielding higher SiO_2 contents [56]. This mechanism uniquely accounts for the ancient crystallization ages of EC 002 (4565.0 ± 0.07 Ma), GRA 06128/9 (4.517 ± 0.060 Ga), and NWA 11119 (4564.8 ± 0.3 Ma), which formed within 2–6 Myr of Solar System inception through low-degree melting of primitive precursors [16,27,28]. The preservation of high-temperature SiO_2 polymorphs (tridymite, cristobalite) and $Mg^{\#}$ values of 50–60 in these samples [34] further attests to rapid ascent and quenching in small-body gravity fields, where limited melt fractions (<10 vol%) were efficiently extracted before extensive fractionation could occur.

Planetary-scale melting (Moon, Vesta, Mars) involved basaltic crustal protoliths and sustained thermal regimes. On the Moon, basaltic underplating of KREEP-enriched lower crust at 0.005–0.05 GPa generated 30–40% partial melts with SiO_2 contents reaching 68 wt% [23]. Mantle plume activity on Mars provided episodic heat flux and decompression melting at similar crustal depths, with magmas potentially containing 0.1–0.5 wt% water to facilitate melting (Sautter et al., 2015). The key distinction from asteroidal cases lies in melt volume and residence time: larger bodies sustained magma chambers that allowed plutonic textures to develop. On Vesta, 10–20% equilibrium partial melting of eucritic crust at 200 bars reproduced DOM 10 dacite compositions [30], demonstrating that even intermediate-sized bodies (525 km) could generate evolved melts through crustal anatexis, though volumetrically minor compared to primary basaltic crust.

Alternative mechanisms face universal mass-balance and geochemical constraints. Fractional crystallization of basaltic magma yields ≤15% residual liquid that accumulates interstitially, producing fine-grained textures inconsistent with the millimeter-scale mineral grains observed in NWA 11119 and ALM-A [16,31]. Silicate liquid immiscibility is further contradicted by trace-element systematics: high-field-strength elements partition preferentially into Fe-rich conjugate melts ($D_{mafic/felsic}$ ~5.6 at 1000 °C), yet observed Th/La ratios in lunar granites and achondrites require incompatible element enrichment in the silicic fraction [23]. This establishes partial melting as the only mechanism capable of generating the observed melt fractions, geochemical systematics, and textural maturity across all extraterrestrial granites.

The universality of partial melting reflects fundamental thermodynamic realities: in anhydrous systems, the high SiO_2 contents (58–77 wt%) and elevated viscosities (10^6–10^9 Pa·s) of granitic melts preclude efficient crystal-liquid separation, making fractionation energetically unfavorable. Consequently, extraterrestrial granites preserve source-region signatures—chondritic for asteroids, basaltic for planets—whereas terrestrial TTGs reflect hydrous melting and garnet fractionation in subduction zones [57]. This mechanistic divergence underscores that partial melting is the default pathway for evolved magma generation in plate tectonics-free environments, with parent body size merely modulating melt volume and extraction efficiency rather than altering the fundamental petrogenetic process.

 doi:10.20944/preprints202601.1308.v1

6.3. Abundance Estimates

Quantifying the true abundance of extraterrestrial evolved lithologies presents a fundamental challenge rooted in non-uniform sampling, preservation biases, and detection limitations. Unlike terrestrial crustal inventories derived from extensive outcrop mapping and seismic profiling, Solar System estimates rely on disproportionately small, fortuitously recovered samples, each unique in mineralogy and provenance, that collectively represent stochastic sampling of ancient, widely disrupted crustal reservoirs [27,28]. This heterogeneity, while demonstrating the ubiquity of evolved magmatism, necessitates a hierarchical approach wherein direct sample measurements provide an absolute lower limit, and systematic bias corrections yield more realistic bounds.

Direct sample-based constraints are starkly limited. The combined mass of ureilite evolved meteorites NWA 11119 and ALM-A totals 477.2 g [16,31], representing merely 0.2% of the ~240 kg global ureilite collection. Similarly, the brachinite GRA 06128/9 (644.5 g) constitutes 1.8% of all brachinites [29], while Apollo 14 regolith studies imply lunar granite comprises 0.5–2% of the lunar crust [20]. Aggregating these disparate metrics suggests an apparent Solar System abundance of 0.2–2% by mass (Figure 4). However, this value must be treated as a severe undersampling artifact rather than a robust estimate, as it reflects neither the original production rates nor the spatial distribution of silicic reservoirs.

Four systematic biases render this baseline a profound underestimate. First, impact ejection efficiency strongly disfavors granite excavation. Numerical models indicate that crater formation preferentially entrains shallow, brittle basaltic crust, whereas deeply seated, high-viscosity granitic plutons (predicted to reside at 10–30 km depth on the Moon) [42] are only sparsely mobilized. Small asteroidal bodies further exacerbate this bias, as their limited gravitational binding energy results in catastrophic disruption rather than selective sampling, destroying silicic crusts rather than ejecting them [31]. Second, atmospheric entry survival imposes a strong mass filter: only robust meteoroids >10 cm diameter typically survive ablation, and the friable, coarse-grained textures of many granitic clasts (e.g., DOM 10) increase breakup probability [30], biasing the flux toward more coherent basaltic material. Third, parent body destruction eliminates source bodies from the modern asteroid belt. The complete spectral disappearance of EC 002's differentiated parent body [27] demonstrates that silicic crusts of numerous early planetesimals were either accreted into larger planets or comminuted to dust via collisional cascade, rendering them invisible to current surveys and meteorite statistics. Finally, detection biases compound these effects: as discussed in Section 4.3, coexisting mafic minerals and space weathering admixture mask felsic spectral signatures, while orbital thermal inertia measurements cannot resolve granite compositions beneath dust-mantled highland surfaces [41].

Synthesizing these factors through an order-of-magnitude estimate suggests the true Solar System abundance may exceed the sample-based lower limit by one to two orders of magnitude. This calculation explicitly acknowledges three key uncertainties. First, the survival rate of silicic crusts on differentiated asteroids after 4.5 Gyr of collisional evolution is poorly constrained; we adopt a conservative range of 0.1–1% based on Bottke et al. (2015), acknowledging that actual values could be higher for larger bodies or those with thicker crusts . Second, impact ejection efficiency represents a severe sampling bias—only ~0.01–0.1% of material from a given depth typically escapes the parent body, with granite plutons at 10–30 km depth being particularly difficult to excavate [58]. Third, atmospheric entry survival further filters the flux, favoring coherent basaltic clasts over friable granitic material by a factor of 10–100. Combining these biases multiplicatively yields a total undersampling factor of 10^3–10^5 relative to original production volumes. Consequently, the apparent 0.2–2% sample-based abundance could correspond to an original production fraction of 1–20% on small bodies, with the broad range reflecting uncertainties in each bias term. For instance, if silicic crusts survived on 5% rather than 1% of asteroids, or if ejection efficiency was 0.5% rather than 0.1%, the estimated production fraction would increase proportionally to 50–100% or decrease to 2–4%, respectively. This sensitivity underscores that our estimate is intended to establish plausibility rather than precision—demonstrating that even conservative bias corrections permit extraterrestrial granite

 doi:10.20944/preprints202601.1308.v1

production at levels comparable to or exceeding those inferred for Hadean Earth (Section 7.1). For planetary-scale bodies, crustal melting models indicate that 5–15% partial melting of basalts, a geologically reasonable flux given mantle plume recurrence intervals of 10^8 years, could generate granitic volumes approaching 10^3–10^4 km^3 per event [23]. Repeated over 500 Myr of early lunar history, such episodic production could yield cumulative abundances of 5–10% within the deep crust, far exceeding the 0.5–2% regolith proportion.

These revised estimates carry direct implications for reconstructing Earth's Hadean crust (Section 7). The same biases—deep-seated residence, spectral masking, and destruction by subsequent tectonism—apply to terrestrial granite preservation, amplifying the significance of extraterrestrial analogues. If the Moon, with its limited radiogenic heat, sustained granitic production at ≥0.5% crustal volume [20], Hadean Earth, with mantle potential temperatures 200 °C higher and continual impact bombardment, could have readily achieved the 0.2–40% felsic inventory inferred from Archean sediment proxies [1]. Ultimately, constraining these abundances requires integrated strategies: targeted sampling of deep crustal exposures in large lunar basins (e.g., South Pole–Aitken) [22], development of thermal infrared spectral indices robust to mafic mixing [21], and in situ Venus surface analysis to assay thickened-plateau melting products. Such efforts will transform our view of evolved magmatism from a planetary curiosity to a quantitatively understood process of Solar System differentiation.

7. Implications for Earth

7.1. Hadean Granites

The Hadean Earth (4.56–4.0 Ga) operated without plate tectonics under a thermal regime propelled by mantle plumes, giant impacts, and radioactive decay of short-lived radionuclides, particularly ^{26}Al [59]. This generated mantle potential temperatures 200–300 ºC above modern values, establishing crustal melting conditions directly analogous to those recorded in the most ancient extraterrestrial granites. NWA 11119, ALM-A, and GRA 06128/9 crystallized within 2–6 Myr of Solar System formation through low-degree (≤30%) partial melting of chondritic protoliths at IW-1.5 to IW-1 [16,27,28], while lunar granites formed via basaltic underplating at 4.37–3.87 Ga [13]. These temporal and mechanistic parallels indicate that Hadean evolved magmatism was governed by similar anhydrous, high-temperature processes, though Earth's greater thermal vigor delivered substantially larger mafic fluxes to the primordial crust [60].

Compositional constraints from detrital Jack Hills zircons (4.4–4.3 Ga) and the ~4.0 Ga Acasta Gneisses reveal that Hadean felsic lithologies contained substantial mafic components, resembling their extraterrestrial counterparts rather than later granitoids. Ti-in-zircon thermometry indicates crystallization temperatures of 680–750 °C [7], consistent with hydrous melting, but the coeval presence of high-Ti, low-Hf zircons suggests thermal excursions to >900 ºC under anhydrous conditions [3]. The systematically Mg-rich compositions of all known terrestrial rocks >4.0 Ga further mandate that Hadean granites incorporated fayalitic olivine and pyroxene, yielding mineral assemblages and flat REE patterns akin to lunar granites or brachinites (Figure 5) [29,60]. These magmas likely exhibited profound textural variability, from quenched volcanic glasses analogous to lunar granophyres to coarse-grained plutonic textures reflecting million-year residence times in transient crustal magma chambers [14,15,27–31]. Emplacement occurred in both intrusive (dikes, sills, shallow plutons) and extrusive (lava domes, impact-triggered eruptions) settings, generating a heterogeneous crustal inventory whose volumetric significance can be constrained through comparative planetary analysis.

Estimating Hadean granite abundance requires integrating lower and upper bounds derived from extraterrestrial analogues and terrestrial geochemical proxies. The lunar regolith constraint of 0.5–2% granite [20] establishes a conservative baseline, as Hadean Earth shared similar anhydrous, plate tectonics-free conditions but possessed substantially higher heat flow from impact bombardment and mantle overturn [59]. However, trace-element systematics in Archean mudstones,

 doi:10.20944/preprints202601.1308.v1

particularly Ni/Co <30 and Cr/Zn <0.1 ratios, suggest Early Archean granite contents of 10–40% [1], which likely represents a plausible Hadean upper bound after accounting for crustal reworking and sedimentary mixing dynamics. Integrating these constraints yields an estimated Hadean felsic inventory of 0.5–40%, implying that granitic lithologies constituted a substantial substrate that may have hosted the earliest prebiotic chemistry, provided the physical template for subsequent Archean continental nucleation, and fundamentally shaped the geochemical architecture of Earth's primordial crust long before plate tectonics transformed granite petrogenesis.

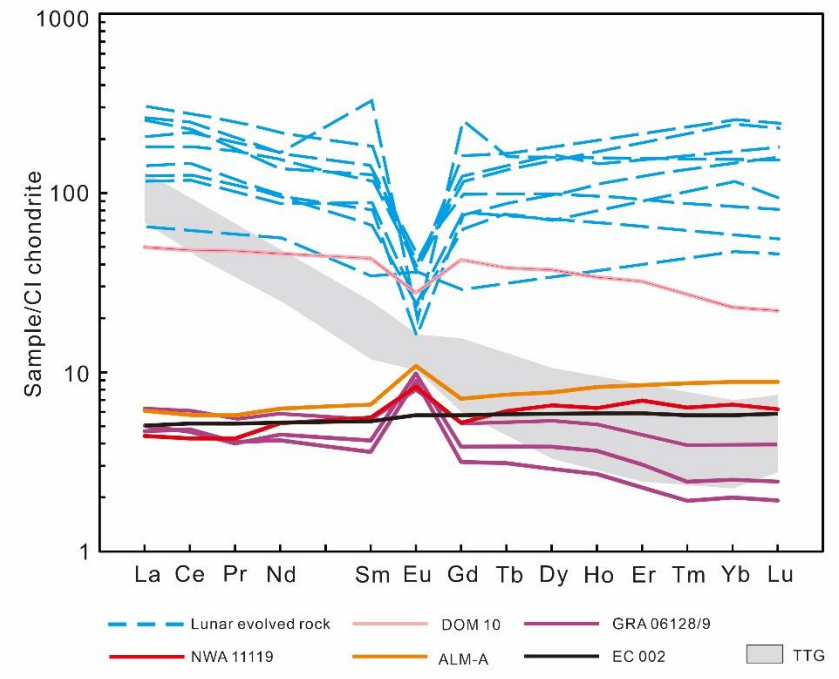

Figure 5. Rare earth element patterns of extraterrestrial evolved rocks compared with the terrestrial Archean TTG field. The plot displays CI-chondrite normalized abundances for lunar granites, asteroidal dacites (DOM 10), and diverse silicic meteorites including NWA 11119, ALM-A, EC 002, and GRA 06128/9. A defining characteristic of these extraterrestrial lithologies is their characteristically flat REE patterns, which lack the pronounced heavy rare earth element depletion diagnostic of Earth's TTG suites (shaded area).

7.2. Archean Granites

The Archean transition marks a fundamental shift from extraterrestrial-style granite production to geodynamic regimes unique to Earth. While Hadean magmatism likely mirrored the anhydrous, mafic-rich, and variably fractionated lithologies preserved in meteorites and lunar samples, Archean tonalite-trondhjemite-granodiorite (TTG) suites and Phanerozoic arc granites represent a profound departure [57]. TTGs are distinguished not merely by their pronounced HREE depletion ($[Dy/Yb]_N$ >1.5) and hydrous mineral assemblages (amphibole, biotite), but by their genesis within tectonic frameworks (subduction or thickened plateau melting) that have no confirmed Solar System analogues [10,61]. This dichotomy underscores that Earth's crustal evolution diverged from the prevailing mode of planetary differentiation, rendering extraterrestrial granites imperfect analogues for post-Hadean terrestrial magmatism yet critical for constraining the primordial baseline.

The subduction-affinity model posits that hydrated oceanic crust melted at garnet-stable depths (>40 km), generating diagnostic HREE depletion through residual garnet retention and requiring plate tectonics and abundant surface water—conditions exclusive to Earth among planetary bodies [3,61]. Conversely, the thickened-plateau model invokes melting of basaltic plateaus underplated by mantle plumes, where gravitational foundering of eclogitic roots drives dehydration melting without subduction [62]. While this plume-driven scenario could operate on any sufficiently large body, its efficacy hinges on sustained thermal fluxes that smaller bodies like the Moon and Vesta could not

 doi:10.20944/preprints202601.1308.v1

maintain [22,30]. Mercury's prolonged magmatism to ~1 Ga suggests greater potential for secondary melting [53], yet its spectrally analogous surface to lunar highlands implies limited felsic production.

Venus emerges as the pivotal test case because its geologically young surface (~500 Ma), sustained plume activity, and ancient hydrated crust create conditions potentially favorable for thickened-plateau melting without subduction. If Venusian highlands represent plateau-related TTG analogues, they would capture the transitional geodynamic regime between anhydrous plutonism and full-fledged plate tectonics. However, orbital spectral limitations and dust mantling preclude definitive assessment: the key question is whether thickened-plateau processes can generate true TTG-like suites—characterized by strong HREE depletion and hydrous mineralogy—without invoking subduction. Resolving this requires in situ geochemical measurements from future Venus lander missions to evaluate whether HREE systematics match the flat patterns of extraterrestrial granites or the fractionated signatures of terrestrial TTGs (Figure 5). Such data would directly constrain whether Earth's Archean transition was primarily catalyzed by plate-tectonic onset or whether thickened-plateau processes alone could bridge Hadean and Archean magmatism.

Synthesis reveals that Earth's Archean granites reflect a singular geodynamic transformation. Early Earth likely hosted a spectrum of granitic lithologies directly analogous to those in meteorites and lunar samples, but the emergence of plate tectonics, whether at 4.0 Ga or later, introduced hydrous melting and garnet stability, generating HREE-depleted TTG suites fundamentally incompatible with anhydrous planetary differentiation [3,10]. Extraterrestrial samples thus provide not a direct analogue for Archean granites, but rather a baseline against which to measure Earth's deviation, a baseline that suggests evolved magmatism is a universal outcome of planetary differentiation. Earth's continents represent a singular, plate-tectonic refinement of this generic process.

8. Conclusion

This review establishes granitic magmatism as a fundamental and pervasive process of planetary differentiation across the Solar System, not uniquely contingent upon Earth's plate tectonics or hydrous melting. Extraterrestrial evolved rocks from the Moon, asteroids, Mars, and potentially Venus document continuous evolved magmatic activity spanning from merely 2.3 Myr after Solar System formation through at least 3.87 Ga, forming under anhydrous conditions via partial melting of mafic crustal sources [13,14,27]. Partial melting of chondritic protoliths generated ancient asteroidal evolved rocks such as EC 002 (4565.0 ± 0.07 Ma) and NWA 11119 (4564.8 ± 0.3 Ma), while basaltic underplating produced younger lunar and Martian examples. These lithologies exhibit distinctive mineralogical and geochemical traits, including nonequilibrium mafic-felsic assemblages, characteristically flat REE patterns devoid of significant HREE depletion, and exceptionally high melt viscosities [16,28], that provide direct analogues for Earth's missing Hadean crustal record and challenge traditional granite paradigms rooted exclusively in terrestrial observations. Current abundance estimates of 0.2–2% for extraterrestrial granite likely represent severe underestimates, being profoundly biased by limited impact ejection efficiencies, spectral masking by coexisting mafic minerals, and atmospheric destruction during meteorite entry [41,45]. This detection-limited perspective implies that Hadean Earth may have hosted between 0.2% and 40% granitic material [1,20], providing a heterogeneous, compositionally variable substrate for prebiotic chemistry and serving as the critical protolith reservoir for subsequent Archean TTG nucleation.

Future breakthroughs in understanding early planetary crustal evolution will require integrated, multi-scale approaches. Priority should be given to sampling deep crustal materials from large impact basins such as the Moon's South Pole–Aitken basin, which could expose ancient plutonic reservoirs inaccessible to prior missions [22]; developing advanced thermal infrared spectral indices capable of remotely detecting felsic lithologies despite mafic mineral mixing and space weathering effects [21]; and conducting systematic high-pressure experiments to quantify melt extraction dynamics and test the viability of partial melting models under variable oxygen fugacity conditions [23,56]. Ultimately, definitive in situ geochemical analysis of Venusian highland terrains, where

 doi:10.20944/preprints202601.1308.v1

orbital data suggest felsic compositions [48] and morphological evidence implies highly viscous silicic magmatism [49], will provide the crucial test for whether thickened-plateau melting generated TTG-like suites beyond Earth. Such investigations will fundamentally reshape our understanding of crustal evolutionary pathways, illuminate the unique geodynamic transformations that produced Earth's continents, and establish whether the emergence of plate tectonics represents the critical divergence point that rendered our planet's granite record truly exceptional in the Solar System.

Funding: This work was supported by the National Natural Science Foundation of China (NSFC) grant (42503028).

Data Availability Statement: The data presented in this study are available in this paper.

Acknowledgments: We sincerely thank reviewer for thorough and constructive comments.

Conflicts of Interest: The authors declare no conflicts of interest.

References

1. Tang, M.; Chen, K.; Rudnick, R.L. Archean Upper Crust Transition from Mafic to Felsic Marks the Onset of Plate Tectonics. *Science.* **2016**, *351*, 372–375, doi:10.1126/science.aad5513.
2. Rollinson, H. There Were No Large Volumes of Felsic Continental Crust in the Early Earth. *Geosphere* **2017**, *13*, 235–246, doi:10.1130/GES01437.1.
3. Turner, S.; Wilde, S.; Wörner, G.; Schaefer, B.; Lai, Y.J. An Andesitic Source for Jack Hills Zircon Supports Onset of Plate Tectonics in the Hadean. *Nat. Commun.* **2020**, *11*, 1–5, doi:10.1038/s41467-020-14857-1.
4. Shang, S.; Lin, Y.; van Westrenen, W.; Brouwer, F.M. Evolution of Magma Compositions and Phosphorus Availability in Early Earth's Crust: New Constraints from Zircon-Melt Partitioning Experiments. *Geology* **2024**, *XX*, 1–5, doi:10.1130/G52304.1.
5. Bonin, B. Extra-Terrestrial Igneous Granites and Related Rocks: A Review of Their Occurrence and Petrogenesis. *Lithos* **2012**, *153*, 3–24, doi:10.1016/j.lithos.2012.04.007.
6. Wilde, S.A.; Valley, J.W.; Peck, W.H.; Graham, C.M. Evidence from Detrital Zircons for the Existence of Continental Crust and Oceans on the Earth 4.4 Gyr Ago. *Nature* **2001**, *409*, 175–178, doi:10.1038/35051550.
7. Harrison, T.M.; Schmitt, A.K. High Sensitivity Mapping of Ti Distributions in Hadean Zircons. *Earth Planet. Sci. Lett.* **2007**, *261*, 9–19, doi:10.1016/j.epsl.2007.05.016.
8. Mojzsis, S.J.; Cates, N.L.; Caro, G.; Trail, D.; Abramov, O.; Guitreau, M.; Blichert-Toft, J.; Hopkins, M.D.; Bleeker, W. Component Geochronology in the Polyphase ca. 3920Ma Acasta Gneiss. *Geochim. Cosmochim. Acta* **2014**, *133*, 68–96, doi:10.1016/j.gca.2014.02.019.
9. Reimink, J.R.; Chacko, T.; Stern, R.A.; Heaman, L.M. Earth's Earliest Evolved Crust Generated in an Iceland-like Setting. *Nat. Geosci.* **2014**, *7*, 529–533, doi:10.1038/ngeo2170.
10. Campbell, I.H.; Taylor, S.R. No Water, No Granites - No Oceans, No Continents. *Geophys. Res. Lett.* **1983**, *10*, 1061–1064, doi:10.1029/GL010i011p01061.
11. Laurent, O.; Martin, H.; Moyen, J.F.; Doucelance, R. The Diversity and Evolution of Late-Archean Granitoids: Evidence for the Onset of "Modern-Style" Plate Tectonics between 3.0 and 2.5 Ga. *Lithos* 2014, *205*, 208–235.
12. Moyen, J.F. The Composite Archaean Grey Gneisses: Petrological Significance, and Evidence for a Non-Unique Tectonic Setting for Archaean Crustal Growth. *Lithos* **2011**, *123*, 21–36, doi:10.1016/j.lithos.2010.09.015.
13. Shih, C.Y.; Nyquist, L.E.; Wiesmann, H. K-Ca Chronology of Lunar Granites. *Geochim. Cosmochim. Acta* **1993**, *57*, 4827–4841, doi:10.1016/0016-7037(93)90202-8.
14. Terada, K.; Bischoff, A. Asteroidal Granite-like Magmatism 4.53 GYR Ago. *Astrophys. J.* **2009**, *699*, 68–71, doi:10.1088/0004-637X/699/2/L68.
15. Beard, A.D.; Downes, H.; Chaussidon, M. Petrology of a Nonindigenous Microgranitic Clast in Polymict Ureilite EET 87720: Evidence for Formation of Evolved Melt on an Unknown Parent Body. *Meteorit. Planet. Sci.* **2015**, *50*, 1613–1623, doi:10.1111/maps.12484.

16. Srinivasan, P.; Dunlap, D.R.; Agee, C.B.; Wadhwa, M.; Coleff, D.; Ziegler, K.; Zeigler, R.; McCubbin, F.M. Silica-Rich Volcanism in the Early Solar System Dated at 4.565 Ga. *Nat. Commun.* **2018**, *9*, 1–8, doi:10.1038/s41467-018-05501-0.
17. Warren, P.H.; Taylor, G.J.; Keil, K.; Shirley, D.N.; Wasson, J.T. Petrology and Chemistry of Two "Large" Granite Clasts from the Moon. *Earth Planet. Sci. Lett.* **1983**, *64*, 175–185, doi:10.1016/0012-821X(83)90202-9.
18. Seddio, S.M.; Jolliff, B.L.; Korotev, R.L.; Zeigler, R.A. Petrology and Geochemistry of Lunar Granite 12032,366-19 and Implications for Lunar Granite Petrogenesis. *Am. Mineral.* **2013**, *98*, 1697–1713, doi:10.2138/am.2013.4330.
19. Warren, P.H. A Concise Compilation of Petrologic Information on Possibly Pristine Nonmare Moon Rocks. *Am. Mineral.* **1993**, *78*, 360–376.
20. Shervais, J.W.; Taylor, L.A. Micrographic Granite: More from Apollo 14. In Proceedings of the Lunar and Planetary Science Conference; 1983; Vol. 14, pp. 696–697.
21. Glotch, T.D.; Lucey, P.G.; Bandfield, J.L.; Greenhagen, B.T.; Thomas, I.R.; Elphic, R.C.; Bowles, N.; Wyatt, M.B.; Allen, C.C.; Hanna, K.D.; et al. Highly Silicic Compositions on the Moon. *Science.* **2010**, *329*, 1510–1513, doi:10.1126/science.1192148.
22. Jolliff, B.L.; Wiseman, S.A.; Lawrence, S.J.; Tran, T.N.; Robinson, M.S.; Sato, H.; Hawke, B.R.; Scholten, F.; Oberst, J.; Hiesinger, H.; et al. Non-Mare Silicic Volcanism on the Lunar Farside at Compton-Belkovich. *Nat. Geosci.* **2011**, *4*, 566–571, doi:10.1038/ngeo1212.
23. Gullikson, A.L.; Hagerty, J.J.; Reid, M.R.; Rapp, J.F.; Draper, D.S. Silicic Lunar Volcanism: Testing the Crustal Melting Model. *Am. Mineral.* **2016**, *101*, 2312–2321, doi:10.2138/am-2016-5619.
24. Arnold, J.R.; Metzger, A.E.; Reedy, R.C. Computer-Generated Maps of Lunar Composition from Gamma Ray Data 1977.
25. Roedder, E.; Weiblen, P.W. Silicate Liquid Immiscibility in Lunar Magmas, Evidenced by Melt Inclusions in Lunar Rocks. *Science.* **1970**, *167*, 641–644, doi:10.1126/science.167.3918.641.
26. Rutherford, M.J.; Hess, P.C.; Daniel, G.H. Experimental Liquid Line of Descent and Liquid Immiscibility for Basalt 70017 GRANITIC MAGMAS in the Lunar Crust Are Indicated by the Occurrence of Granite. *Lunar Planet. Sci. Conf. Proc.* **1974**, *I*, 569–583.
27. Barrat, J.A.; Chaussidon, M.; Yamaguchi, A.; Beck, P.; Villeneuve, J.; Byrne, D.J.; Broadley, M.W.; Marty, B. A 4,565-My-Old Andesite from an Extinct Chondritic Protoplanet. *Proc. Natl. Acad. Sci. U. S. A.* **2021**, *118*, 1–7, doi:10.1073/pnas.2026129118.
28. Day, J.M.D.; Ash, R.D.; Liu, Y.; Bellucci, J.J.; Rumble, D.; McDonough, W.F.; Walker, R.J.; Taylor, L.A. Early Formation of Evolved Asteroidal Crust. *Nature* **2009**, *457*, 179–182, doi:10.1038/nature07651.
29. Day, J.M.D.; Walker, R.J.; Ash, R.D.; Liu, Y.; Rumble, D.; Irving, A.J.; Goodrich, C.A.; Tait, K.; McDonough, W.F.; Taylor, L.A. Origin of Felsic Achondrites Graves Nunataks 06128 and 06129, and Ultramafic Brachinites and Brachinite-like Achondrites by Partial Melting of Volatile-Rich Primitive Parent Bodies. *Geochim. Cosmochim. Acta* **2012**, *81*, 94–128, doi:10.1016/j.gca.2011.12.017.
30. Hahn, T.M.; Lunning, N.G.; McSween, H.Y.; Bodnar, R.J.; Taylor, L.A. Dacite Formation on Vesta: Partial Melting of the Eucritic Crust. *Meteorit. Planet. Sci.* **2017**, *52*, 1173–1196, doi:10.1111/maps.12870.
31. Bischoff, A.; Horstmann, M.; Barrat, J.A.; Chaussidon, M.; Pack, A.; Herwartz, D.; Ward, D.; Vollmer, C.; Decker, S. Trachyandesitic Volcanism in the Early Solar System. *Proc. Natl. Acad. Sci. U. S. A.* **2014**, *111*, 12689–12692, doi:10.1073/pnas.1404799111.
32. Bischoff, A. Mineralogy, Chemistry and Noble Gas Contents of Adzhi-Bogdo - an LL3- 6 Chondritic Breccia with L-Chondrite and Granitoidal Clasts. *Meteoritics* **1993**, *28*, 570–578, doi:10.1111/j.1945-5100.1993.tb00280.x.
33. Sokol, A.K.; Mezger, K.; Chaussidon, M.; Bischoff, A. *Achondritic Fragments in Ordinary Chondrite Breccias*; 2007; Vol. 42;.
34. Nicklas, R.W.; Day, J.M.D.; Gardner-Vandy, K.G.; Udry, A. Early Silicic Magmatism on a Differentiated Asteroid. *Nat. Geosci.* **2022**, *15*, 696–699, doi:10.1038/s41561-022-00996-1.
35. Santos, A.R.; Agee, C.B.; McCubbin, F.M.; Shearer, C.K.; Burger, P. V.; Tartèse, R.; Anand, M. Petrology of Igneous Clasts in Northwest Africa 7034: Implications for the Petrologic Diversity of the Martian Crust. *Geochim. Cosmochim. Acta* **2015**, *157*, 56–85, doi:10.1016/j.gca.2015.02.023.

36. Hewins, R.H.; Zanda, B.; Humayun, M.; Nemchin, A.; Lorand, J.P.; Pont, S.; Deldicque, D.; Bellucci, J.J.; Beck, P.; Leroux, H.; et al. Regolith Breccia Northwest Africa 7533: Mineralogy and Petrology with Implications for Early Mars. *Meteorit. Planet. Sci.* **2017**, *52*, 89–124, doi:10.1111/maps.12740.
37. Lindner, M.; Schmitt, A.K.; Krot, A.N.; Brenker, F.E. Rhyolitic (Micrographic Granite) Igneous Clasts from Ancient Mars in Meteorite Northwest Africa 8171. *Lunar Planet. Sci. Conf.* **2020**, *3*, 1382, doi:10.46427/gold2020.1570.
38. Malarewicz, V.; Beyssac, O.; Zanda, B.; Marin-Carbonne, J.; Leroux, H.; Rubatto, D.; Bouvier, A.S.; Deldicque, D.; Pont, S.; Bernard, S.; et al. Evidence for Pre-Noachian Granitic Rocks on Mars from Quartz in Meteorite NWA 7533. *Nat. Geosci.* **2025**, *18*, 207–212, doi:10.1038/s41561-025-01653-z.
39. Bouvier, L.C.; Costa, M.M.; Connelly, J.N.; Jensen, N.K.; Wielandt, D.; Storey, M.; Nemchin, A.A.; Whitehouse, M.J.; Snape, J.F.; Bellucci, J.J.; et al. Evidence for Extremely Rapid Magma Ocean Crystallization and Crust Formation on Mars. *Nature* **2018**, *558*, 586–589, doi:10.1038/s41586-018-0222-z.
40. Sautter, V.; Toplis, M.J.; Wiens, R.C.; Cousin, A.; Fabre, C.; Gasnault, O.; Maurice, S.; Forni, O.; Lasue, J.; Ollila, A.; et al. In Situ Evidence for Continental Crust on Early Mars. *Nat. Geosci.* **2015**, *8*, 605–609, doi:10.1038/ngeo2474.
41. Sautter, V.; Toplis, M.J.; Beck, P.; Mangold, N.; Wiens, R.; Pinet, P.; Cousin, A.; Maurice, S.; LeDeit, L.; Hewins, R.; et al. Magmatic Complexity on Early Mars as Seen through a Combination of Orbital, in-Situ and Meteorite Data. *Lithos* **2016**, *254–255*, 36–52, doi:10.1016/j.lithos.2016.02.023.
42. Wieczorek, M.A.; Zuber, M.T. Thickness of the Martian Crust: Improved Constraints from Geoid-to-Topography Ratios. *J. Geophys. Res. E Planets* **2004**, *109*, 1–16, doi:10.1029/2003je002153.
43. Baratoux, D.; Samuel, H.; Michaut, C.; Toplis, M.J.; Monnereau, M.; Wieczorek, M.; Garcia, R.; Kurita, K. Petrological Constraints on the Density of the Martian Crust. *J. Geophys. Res. Planets* **2014**, *119*, 1707–1727, doi:10.1002/2014JE004642.
44. Christensen, P.R.; McSween, H.Y.; Bandfield, J.L.; Ruff, S.W.; Rogers, A.D.; Hamilton, V.E.; Gorelick, N.; Wyatt, M.B.; Jakosky, B.M.; Kieffer, H.H.; et al. Evidence for Magmatic Evolution and Diversity on Mars from Infrared Observations. *Nature* **2005**, *436*, 504–509, doi:10.1038/nature03639.
45. Wray, J.J.; Hansen, S.T.; Dufek, J.; Swayze, G.A.; Murchie, S.L.; Seelos, F.P.; Skok, J.R.; Irwin, R.P.; Ghiorso, M.S. Prolonged Magmatic Activity on Mars Inferred from the Detection of Felsic Rocks. *Nat. Geosci.* **2013**, *6*, 1013–1017, doi:10.1038/ngeo1994.
46. Namiki, N.; Solomon, S.C. Impact Crater Densities on Volcanoes and Coronae on Venus: Implications for Volcanic Resurfacing. *Science.* **1994**, *265*, 929–933, doi:10.1126/science.265.5174.929.
47. Gülcher, A.J.P.; Gerya, T. V.; Montési, L.G.J.; Munch, J. Corona Structures Driven by Plume–Lithosphere Interactions and Evidence for Ongoing Plume Activity on Venus. *Nat. Geosci.* **2020**, *13*, 547–554, doi:10.1038/s41561-020-0606-1.
48. Hashimoto, G.L.; Roos-Serote, M.; Sugita, S.; Gilmore, M.S.; Kamp, L.W.; Carlson, R.W.; Baines, K.H. Felsic Highland Crust on Venus Suggested by Galileo Near-Infrared Mapping Spectrometer Data. *J. Geophys. Res. E Planets* **2009**, *114*, 1–10, doi:10.1029/2008JE003134.
49. Ivanov, M.A.; Head, J.W. Stratigraphic and Geographic Distribution of Steep-Sided Domes on Venus: Preliminary Results from Regional Geological Mapping and Implications for Their Origin. *J. Geophys. Res. E Planets* **1999**, *104*, 18907–18924, doi:10.1029/1999JE001039.
50. Petford, N. Dyke Widths and Ascents Rates of Silicic Magmas on Venus. *Trans. R. Soc. Edinburgh, Earth Sci.* **2000**, *91*, 87–95, doi:10.1017/s0263593300007318.
51. Kargel, J.S.; Komatsu, G.; Baker, V.R.; Strom, R.G. The Volcanology of Venera and VEGA Landing Sites and the Geochemistry of Venus. *Icarus* **1993**, *103*, 253–275, doi:10.1006/icar.1993.1069.
52. Abdrakhimov, A.M.; Basilevsky, A.T. Geology of the Venera and Vega Landing-Site Regions. *Sol. Syst. Res.* **2002**, *36*, 136–159, doi:10.1023/A:1015222316518.
53. Massironi, M.; Cremonese, G.; Marchi, S.; Martellato, E.; Mottola, S.; Wagner, R.J. Mercury's Geochronology Revised by Applying Model Production Function to Mariner 10 Data: Geological Implications. *Geophys. Res. Lett.* **2009**, *36*, 1–6, doi:10.1029/2009GL040353.
54. Solomon, S.C. Mercury: The Enigmatic Innermost Planet. *Earth Planet. Sci. Lett.* **2003**, *216*, 441–455, doi:10.1016/S0012-821X(03)00546-6.

55. Filiberto, J.; Chin, E.; Day, J.M.D.; Franchi, I.A.; Greenwood, R.C.; Gross, J.; Penniston-Dorland, S.C.; Schwenzer, S.P.; Treiman, A.H. Geochemistry of Intermediate Olivine-Phyric Shergottite Northwest Africa 6234, with Similarities to Basaltic Shergottite Northwest Africa 480 and Olivine-Phyric Shergottite Northwest Africa 2990. *Meteorit. Planet. Sci.* **2012**, *47*, 1256–1273, doi:10.1111/j.1945-5100.2012.01382.x.
56. Collinet, M.; Grove, T.L. Widespread Production of Silica- and Alkali-Rich Melts at the Onset of Planetesimal Melting. *Geochim. Cosmochim. Acta* **2020**, *277*, 334–357, doi:10.1016/j.gca.2020.03.005.
57. Moyen, J.F.; Martin, H. Forty Years of TTG Research. *Lithos* **2012**, *148*, 312–336, doi:10.1016/j.lithos.2012.06.010.
58. Bottke, W.F.; Vokrouhlický, D.; Marchi, S.; Swindle, T.; Scott, E.R.D.; Weirich, J.R.; Levison, H. Dating the Moon-Forming Impact Event with Asteroidal Meteorites. *Science.* **2015**, *348*, 321–323, doi:10.1126/science.aaa0602.
59. Herzberg, C.; Rudnick, R. Formation of Cratonic Lithosphere: An Integrated Thermal and Petrological Model. *Lithos* **2012**, *149*, 4–15, doi:10.1016/j.lithos.2012.01.010.
60. Keller, C.B.; Harrison, T.M. Constraining Crustal Silica on Ancient Earth. *Proc. Natl. Acad. Sci. U. S. A.* **2020**, *117*, 21101–21107, doi:10.1073/pnas.2009431117.
61. Ge, R.; Zhu, W.; Wilde, S.A.; Wu, H. Remnants of Eoarchean Continental Crust Derived from a Subducted Proto-Arc. *Sci. Adv.* **2018**, *4*, eaao3159, doi:10.1126/sciadv.aao3159.
62. Bédard, J.H. A Catalytic Delamination-Driven Model for Coupled Genesis of Archaean Crust and Sub-Continental Lithospheric Mantle. *Geochim. Cosmochim. Acta* **2006**, *70*, 1188–1214, doi:10.1016/j.gca.2005.11.008.